BMC Genomics

RESEARCH Open Access

Intercellular crosstalk in adult dental pulp is mediated by heparin-binding growth factors Pleiotrophin and Midkine

Natnicha Jiravejchakul[1,2], Gabriela L. Abe[3*], Martin Loza[4], Soyoung Park[5], Ponpan Matangkasombut[2], Jun-Ichi Sasaki[6], Satoshi Imazato[3,6], Diego Diez[7] and Daron M. Standley[1,5*]

Abstract

Background In-depth knowledge of the cellular and molecular composition of dental pulp (DP) and the crosstalk between DP cells that drive tissue homeostasis are not well understood. To address these questions, we performed a comparative analysis of publicly available single-cell transcriptomes of healthy adult human DP to 5 other reference tissues: peripheral blood mononuclear cells, bone marrow, adipose tissue, lung, and skin.

Results Our analysis revealed that DP resident cells have a unique gene expression profile when compared to the reference tissues, and that DP fibroblasts are the main cell type contributing to this expression profile. Genes coding for pleiotrophin (*PTN*) and midkine (*MDK*), homologous heparin-binding growth-factors, possessed the highest differential expression levels in DP fibroblasts. In addition, we identified extensive crosstalk between DP fibroblasts and several other DP resident cells, including Schwann cells, mesenchymal stem cells and odontoblasts, mediated by *PTN* and *MDK*.

Conclusions DP fibroblasts emerge as unappreciated players in DP homeostasis, mainly through their crosstalk with glial cells. These findings suggest that fibroblast-derived growth factors possess major regulatory functions and thus have a potential role as dental therapeutic targets.

Keywords Dental Pulp, Single-cell analysis, RNA-seq, Transcriptome, Fibroblasts, Pleiotrophin, Midkine, Homeostasis, Paracrine communication

*Correspondence:
Gabriela L. Abe
abe.gabriela.dent@osaka-u.ac.jp
Daron M. Standley
standley@ifrec.osaka-u.ac.jp
[1]Department of Genome Informatics, Research Institute for Microbial Diseases, Osaka University, 3-1 Yamadaoka, Suita 565-0871, Japan
[2]Department of Microbiology, Faculty of Science, Mahidol University, Bangkok 10400, Thailand
[3]Department of Advanced Functional Materials Science, Osaka University Graduate School of Dentistry, 1-8 Yamadaoka, Suita 565-0871, Japan
[4]Laboratory of Functional Analysis in silico, Human Genome Center, The Institute of Medical Science, The University of Tokyo, 4-6-1 Shirokane-dai, Minato-ku, Tokyo 108- 8639, Japan
[5]Department of Systems Immunology, Immunology Frontier Research Center, Osaka University, 3-1 Yamadaoka, Suita 565-0871, Japan
[6]Department of Dental Biomaterials, Osaka University Graduate School of Dentistry, 1-8 Yamadaoka, Suita 565-0871, Japan
[7]Quantitative Immunology Research Unit, Immunology Frontier Research Center, Osaka University, 3-1 Yamadaoka, Suita 565-0871, Japan

Introduction

Dental pulp (DP) is a soft tissue of ectomesenchymal origin, located within teeth, and surrounded by rigid dentine walls. Vascularization and innervation are supplied through the apical foramen, a narrow opening at the end of each dental root. This anatomical configuration often makes relatively minor inflammation result in severe pain and tissue necrosis, by strictly limiting tissue swelling and increasing internal pressure. If tissue vitality is preserved, then damaged tissue can be recovered by the regenerative abilities of DP. DP regenerates by recruiting the same cell types involved in homeostasis, and no new cell type that is unique to injury has been observed [1, 2]. Although DP tissue repair can be promoted by various dental treatments such as pulp capping, few interventions harness its regenerative properties. Currently, the composition of DP at the cellular and molecular levels, as well as the mechanisms by which DP resident cells maintain homeostasis, are not well understood.

Several studies have reported interactions among cells in DP, with special attention given to mesenchymal stem cells (MSCs) and their niches [3, 4]. It is now accepted that DP possesses two main MSCs niches, perivascular and neural, which participate in tissue development and regeneration [5]. Within these niches, mechanisms of self-regulation have been discovered. However, it is not clear how other resident and transient cells interact with these niches or participate in the regulation of overall tissue homeostasis.

Single-cell transcriptomics allows the quantification of gene expression in individual cells in a tissue sample. Recent analysis of human DP have identified cells involved in tissue development [1], delineated major cellular components of adult DP [6], and described enriched cell types under carious lesion conditions [7].

Here, we sought to characterize DP tissue at the cellular and molecular levels by integrating the data from all publicly available healthy human DP single-cell transcriptome datasets. As a reference, we integrated data from five different human tissues of healthy adults. We hypothesized that the gene expression patterns in DP cells would be distinct from those in the corresponding cell types in reference tissues. We further reasoned that, if such unique phenotypes were observed, they would help shed light on the biological processes responsible for DP tissue homeostasis. Such insight may further inform the development of cellular and molecular-based treatment strategies in dentistry.

Results

DP resident fibroblasts exhibit unique gene expression profiles

The cell composition of and transcriptomic signatures within DP tissues were investigated by integrating nine DP single-cell RNA sequencing datasets with ten datasets from five reference tissues: peripheral blood mononuclear cells (PBMC), bone marrow (BM), adipose tissue (ADP), lung (LUNG), and skin (SKIN). We selected these tissues because they contain representatives of the major cell types populating the DP [5, 8]. After applying all QC filters, the resulting dataset contained 109,554 cells, and 33,401 genes, including 48,659 cells from DP and 60,895 from other tissues (Fig. 1a). Clustering identified nineteen distinct cell clusters which were further annotated by cell type (Fig. 1b) (Supplementary Fig. 1a) using established markers from the literature along with CellTypist encyclopedia [9] (Supplementary Fig. 1b). Overall, fibroblasts which were identified by the expression of markers *COL1A1*, *COL1A2*, *COL3A1*, *DCN*, and *CXCL14* (Fig. 1c), were the most abundant cell type. We found a very small cluster of *MKI67*+proliferating fibroblasts (pro-fibroblasts) (Cluster18) that was present only in skin tissue (Fig. 1d). Schwann cells (Schw), which consisted of myelinated Schw (*MBP*+) and non-myelinated Schw (*GFRA3*+) were identified by the expression of *SOX10* [10, 11] (Supplementary Fig. 2). DP was enriched in both fibroblasts and Schw clusters (Fig. 1d). In addition, a small cluster of odontoblasts was identified by the expression of *DMP1* (Fig. 1b) (Supplementary Fig. 3). Other cells identified included immune cells (cluster 8, 13, 15, 1, and 14), endothelial cells (clusters 6 and 12), epithelial cells and keratinocytes (cluster 16). Finally, two clusters (5 and 10) with markers compatible with perivascular cells (*CSPG4*) [12], including vascular smooth muscle cells (*ACTA2*, *TAGLN*, and *TPM2*) [13, 14], and mesenchymal stem cells (*ACTA2*, *FRZB*, *NOTCH3*, and *MYH11*) [6, 12] were annotated as MSC-like cells (Supplementary Fig. 4).

To identify tissue-specific features, we performed PCA for each cell cluster in Fig. 1b using average expression profiles (pseudo-bulk) for each sample. The corresponding plots showing the pseudo-bulk sample distribution in the first 2 principal components (PCs) of all clusters are shown in Supplementary Fig. 5. The PCA plots indicated that DP fibroblasts (Cluster 0, 2, 3, and 7) and Schwann cells (Cluster 9 and 11) were well separated from those of other reference tissues, suggesting the existence of DP specific markers driving this separation (Supplementary Fig. 5).

In order to understand the gene expression signatures unique to DP fibroblasts, we performed PCA on pseudo-bulk signatures using cells in the fibroblast clusters (0, 2, 3 and 7). For this analysis, proliferating fibroblasts (cluster 18) were not included, as they were found only in skin. The first two components (PC1 and PC2) showed separation between fibroblasts from DP compared to fibroblasts from other tissues (Fig. 1e). Then, the top 500 genes contributing to PC1 and PC2 were obtained and used to

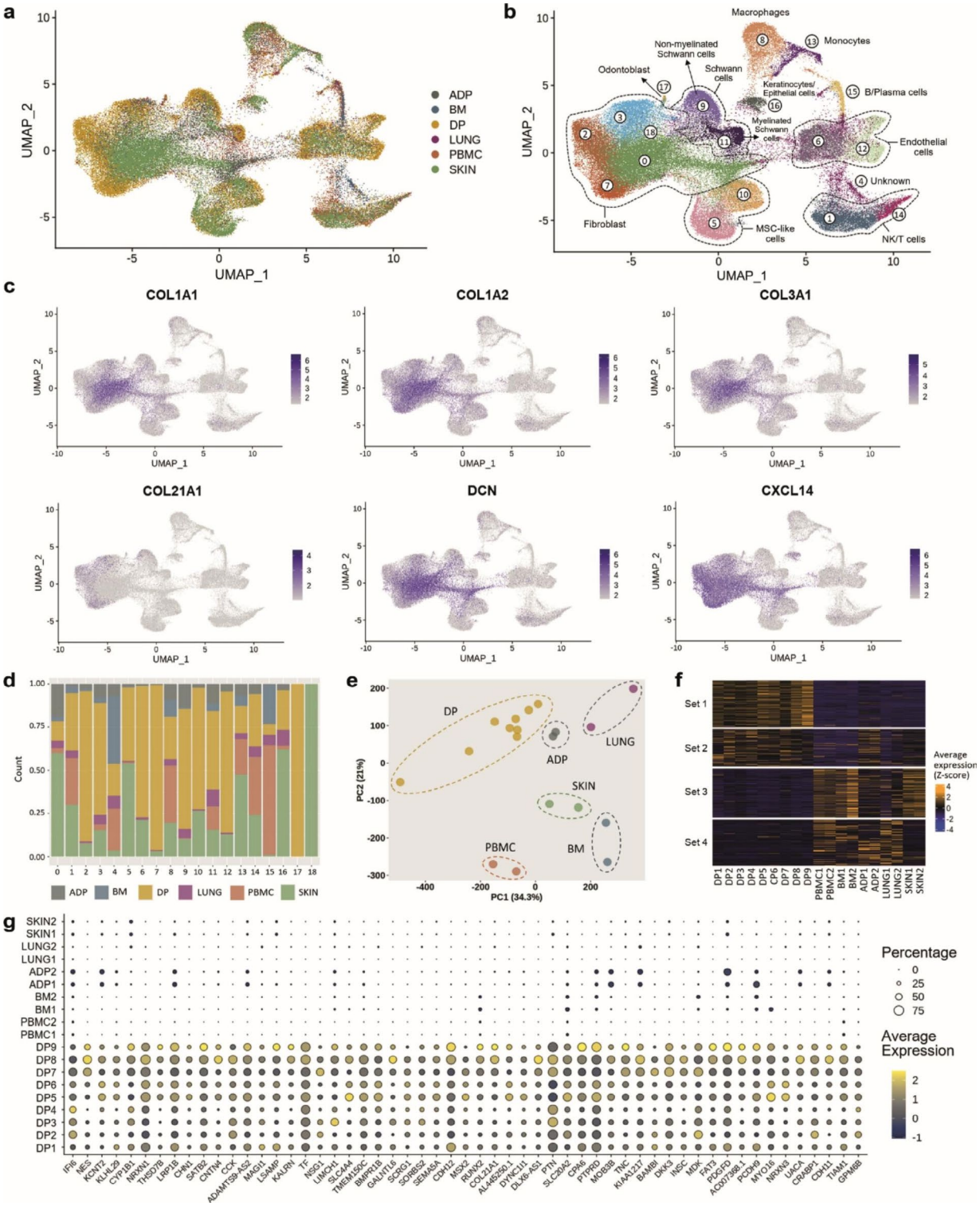

Fig. 1 scRNA-seq analysis of human dental pulp and reference tissues from healthy adults. (**a**) UMAP visualization of all integrated tissues, cell clusters are colored by tissue of origin. (**b**) UMAP visualization of unbiased cluster classification identifying 19 cell clusters with cell type annotation. (**c**) Feature plots of fibroblast markers identifying the cell population within clusters 0, 2, 3, 7 and 18. (**d**) Bar plot of the fraction of cells that compose each cluster shown in **c**, colored by tissue of origin. (**e**) Principal component analysis plot of fibroblasts performed using average gene expression for each sample. (**f**) Heatmap of the top 500 differentially expressed genes that contributed to PC1 and PC2 in **e**, set 1 shows upregulated genes in DP fibroblasts. (**g**) Dot plot of curated genes of interest retrieved from heatmap set 1, the complete list of genes is provided in Supplementary Table 1

construct a heatmap (Fig. 1f). The heatmap highlighted a group of genes (set 1) as being upregulated in DP fibroblasts while downregulated in fibroblasts of other reference tissues. We further curated genes from the heatmap set 1 to construct a dot plot with genes of interest showing the highest average expression in DP (Fig. 1g) (a complete list of genes retrieved from heatmap set 1 is provided in Supplementary Table 1). Taken together, our analyses revealed that DP have a unique gene expression profile when compared to the five reference tissues and that DP fibroblasts are the main contributors to these features.

Heparin-binding growth factors pleiotrophin (PTN) and midkine (MDK) are highly expressed in DP resident fibroblasts

To gain insight into DP fibroblast specific genes at single-cell resolution, we next compared the differential gene expression between DP fibroblasts and those from reference tissues. The volcano plot in Fig. 2a highlights genes

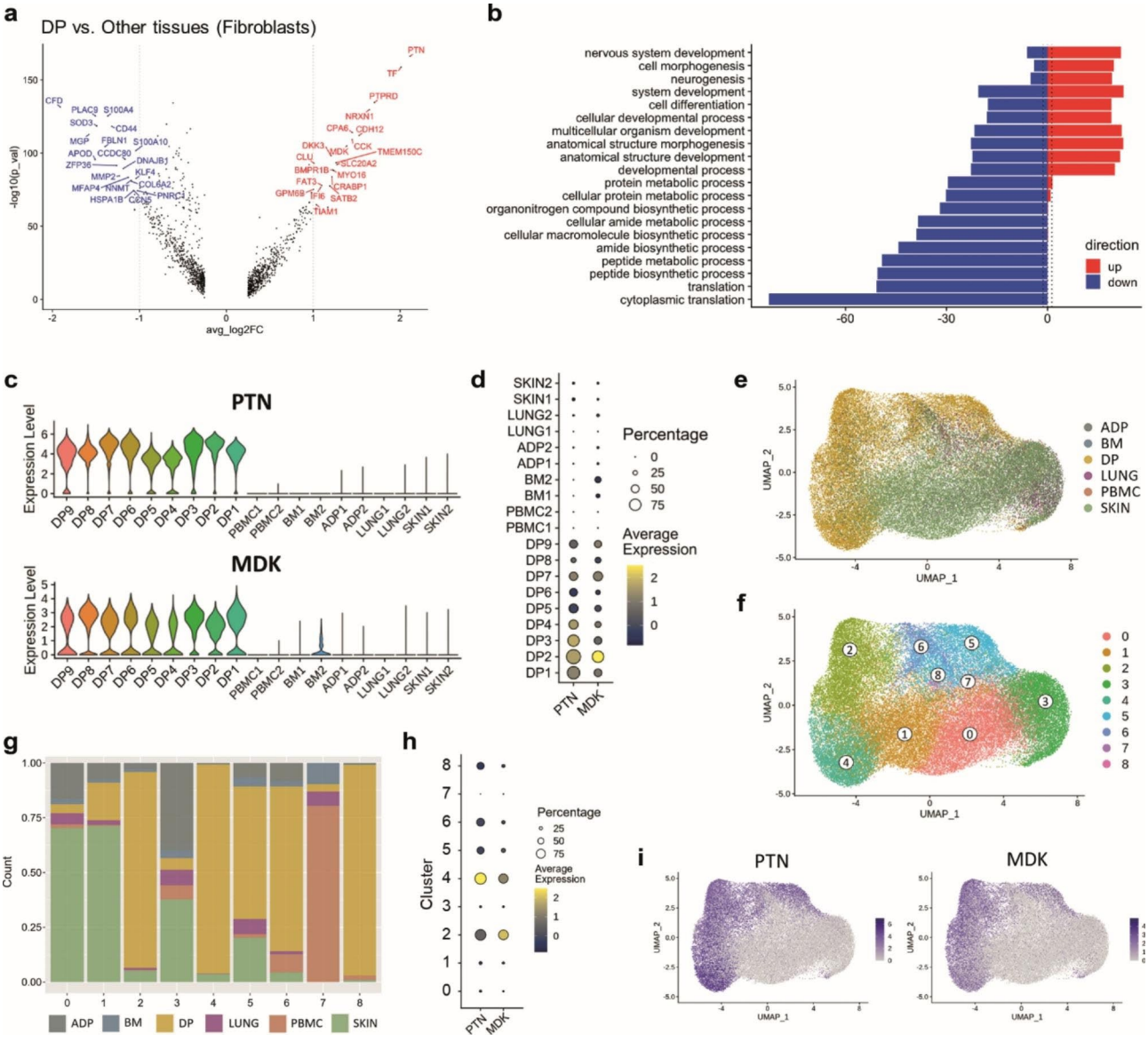

Fig. 2 Dental pulp fibroblasts versus those from reference tissues. (**a**) *PTN* and *MDK* are differentially expressed genes in DP fibroblast versus reference tissue fibroblasts. (**b**) Gene ontology enrichment analysis using the DE genes from **a** identified significantly upregulated Biological Processes in DP fibroblasts. (**c**) Violin plots of *PTN* (upper) and *MDK* (lower) expression levels in fibroblasts of all tissues. (**d**) Dot plot showing percentage and average expression of *PTN* and *MDK* of fibroblasts of all tissues. (**e**) UMAP visualization of fibroblasts from all tissues integrated and colored by tissue of origin. (**f**) Unbiased classification identifying 9 clusters of fibroblast sup-populations. (**g**) Bar plot of the fraction of cells that compose each cluster shown in **f**, colored by tissue of origin. (**h**) Expression of *PTN* (upper) and *MDK* (lower) projected onto the UMAP plot of integrated fibroblasts. (**i**) Dot plot showing percentage and average expression of *PTN* and *MDK* by clusters of fibroblasts in **f**

with large fold changes that are also statistically significant. The eight most elevated genes in DP fibroblasts were *PTN*, *TF*, *PTPRD*, *NRXN1*, *CDH12*, *CCK*, *CPA6*, and *MDK* (Fig. 2a), consistent with the genes retrieved from PCA pseudo-bulk analysis shown in Fig. 1g. We next performed gene set enrichment analysis to investigate which gene ontology (GO) terms were under- or over-represented in these genes. The top GO terms in the Biological Process ontology were: "nervous system development", "cell morphogenesis", "neurogenesis", "system development" and "cell differentiation" (Fig. 2b).

Within the DE genes in Fig. 2a, *PTN*–the most upregulated gene in DP fibroblasts–and *MDK*, are homologs coding for Pleiotrophin and Midkine, respectively. *PTN* and *MDK* are members of a distinct family of secreted heparin-binding growth factors that have been implicated in various biological processes, from development to inflammation to tumorigenesis [15]. We found that *PTN* and *MDK* were highly expressed in all nine DP datasets, while their levels were extremely low in all ten datasets from the other five reference tissues (Fig. 2c, d).

To further investigate the unique contribution of *PTN* and *MDK* to DP fibroblasts, fibroblast clusters from all six tissues were independently integrated, and UMAP coordinates and clusters were recalculated, resulting in nine subpopulations (Fig. 2e, f). Fibroblast clusters 2, 4, 5, 6 and 8 were enriched significantly in DP tissues (Fig. 2g). As expected, *PTN* and *MDK* were expressed only in these DP-resident fibroblast clusters (Fig. 2h, i), confirming that *PTN* and *MDK* are the key genes distinguishing the DP fibroblasts from the reference tissue fibroblasts.

Analysis of DP cell populations and PTN- and MDK-mediated intercellular communication networks

To understand the biological relevance of *PTN* and *MDK* in the DP environment, we next ignored the reference tissues and turned our attention exclusively to the DP datasets. Data integration of all nine healthy DP datasets retrieved from three different studies (Supplementary Table 2) was performed. Unbiased clustering predicted nineteen different clusters, which were further grouped into eleven cell types (Fig. 3a) using known markers indicated in Fig. 3b. Our results revealed that fibroblasts were the largest cell population in the dental pulp (43.92%), followed by endothelial cells (18.05%), MSCs (13.79%) and Schwann cells (12.39%) when combining non-myelinated and myelinated cells. While B cells and erythrocytes were the smallest cell cluster (0.4%) (Fig. 3c). As expected, elevation of *PTN* and *MDK* expression was found in clusters annotated as fibroblasts (Fig. 3d).

Since *PTN* and *MDK* are secreted heparin-binding molecules, we sought to investigate potential target cells based on the mRNA expression of their known receptors using CellPhoneDB[16]. Our analysis revealed a high number of overall interactions between fibroblasts and non-myelinated Schwann cells, MSCs, endothelial cells and odontoblasts (Fig. 4a), including interactions independent of *PTN* or *MDK*. To illustrate specific ligand-receptor pairs contributing to these interactions between fibroblasts and other cell types, chord diagrams were constructed using the top twenty-five interacting pairs (Fig. 4b). It is shown that *PTN* and *MDK* were the top molecules mediating major communication between fibroblasts and non-myelinated Schwann cells, MSCs and odontoblasts, but not endothelial cells (Fig. 4b, Supplementary Fig. 6). In addition, even though fibroblast interacted with several DP cells via *PTN* and *MDK*, the prediction for their receptors varied depending on the cell type (Fig. 4b, Supplementary Fig. 6).

PTN and *MDK* bind both heparin and heparan sulfate (HS). These are linear polysaccharides attached to cell surfaces by one or more anchoring proteins. In order to further support the role of *PTN*- and *MDK*-mediated communication between DP fibroblasts and various other DP resident cells, we next investigated the expression levels of genes encoding major HS anchor proteins. We found *BGN*, *GPC3*, *SDC2* were expressed on cells that also expressed high levels of receptors for *PTN* and *MDK* (Supplementary Fig. 7a). In addition, we determined the expression of genes involved in the biosynthesis of HS itself (Supplementary Fig. 7b). Taken together, these results support a model where *PTN* and *MDK* are produced by DP-resident fibroblasts and exert a paracrine effect on several types of DP cells, most significantly Schwann cells and odontoblasts.

Discussion

In order to characterize DP tissue homeostasis, we integrated all publicly available scRNA-seq data from healthy human DP and compared the expression profiles with several well-studied reference tissues. We hypothesized that, due to the unique functional constraints on DP cells, their gene expression patterns would be distinct from those of other tissues. Our analysis revealed that DP tissue indeed exhibited a unique gene expression profile in comparison to reference tissues and that DP resident fibroblasts are the source of these differences.

Other cellular components of the tissues studied here, such as endothelial cells and immune cells, did not show significant differences, suggesting a common behavior across those tissues. While fibroblasts are found throughout the human body, their function is dependent on local environment and context to support other resident cells and engage in tissue remodeling when necessary [17]. In our study, we evaluated data obtained from healthy adult DP tissues, and assumed a context of steady state and homeostasis. A total of six subpopulations of fibroblasts were identified, revealing a previously unappreciated

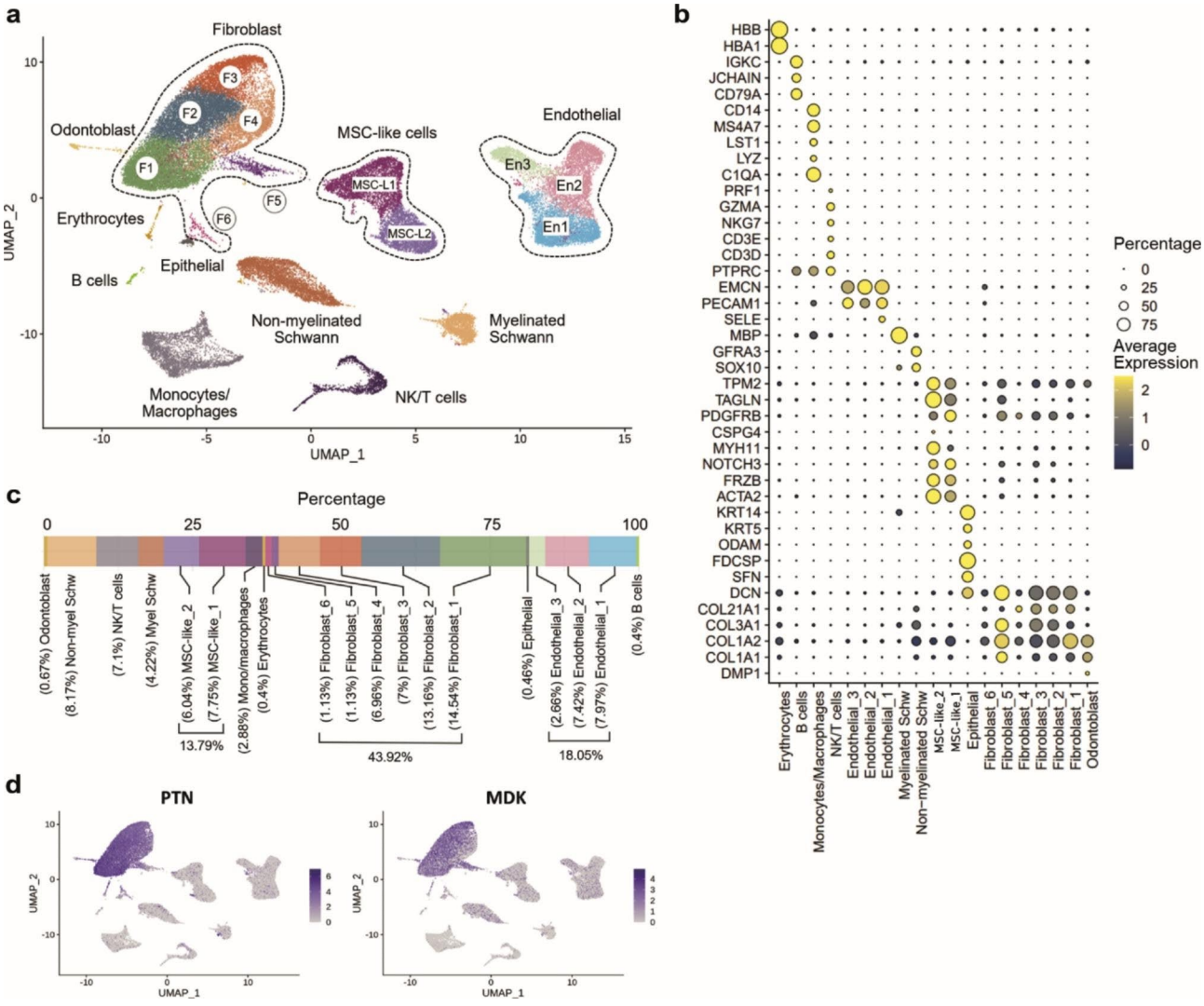

Fig. 3 ScRNA-seq analysis of integrated human dental pulp tissues. (**a**) UMAP visualization of integrated DP datasets. (**b**) Expression levels of known cell type markers used for the cluster annotation in **a**. (**c**) Percentage of cell types that compose the healthy adult human DP. (**d**) Expression of *PTN* (left) and *MDK* (right) projected onto the UMAP plot of integrated dental pulp tissues, fibroblasts highly express *PTN* and *MDK*.

diversity, suggesting that each distinct fibroblast subtype within DP may be involved in distinct functional roles. Characterization of these subpopulations is now necessary and particular attention should be placed on the identification of non-overlapping functions, as these may be used to develop new therapeutics.

Studies on single-cell analysis of human DP are few, and their methodologies differ both in sequencing platform and chemistry. To minimize batch effects in our analysis we selected only studies that used equivalent and most current methodology, ignoring those that used different platforms. However, our results largely agree with previously published data, regardless of their methodology. Yin et al. identified similar cell types as were observed here; a cluster labeled "pulp cells"–which can be regarded as fibroblasts given their expressed markers–showed an active communication network with other cells in the DP [18]. MSCs were found to be the main cluster interacting with fibroblasts; however, in addition to MSCs, we show that fibroblasts have significant interactions with Schwann cells, endothelial cells and odontoblasts. Our integrative approach, that included multiple datasets from the literature, yielded a greater number of cells than any individual study capturing additional significant interactions in the communication networks within cell clusters.

Our analysis identified several functional genes contributing to the unique expression profile of DP-resident fibroblasts: Transferrin (*TF*), reported to support tooth morphogenesis and dental cell differentiation [19]; Cadherin 12 (*CDH12*), which plays an important role in calcium-dependent cell adhesion and has been implicated in

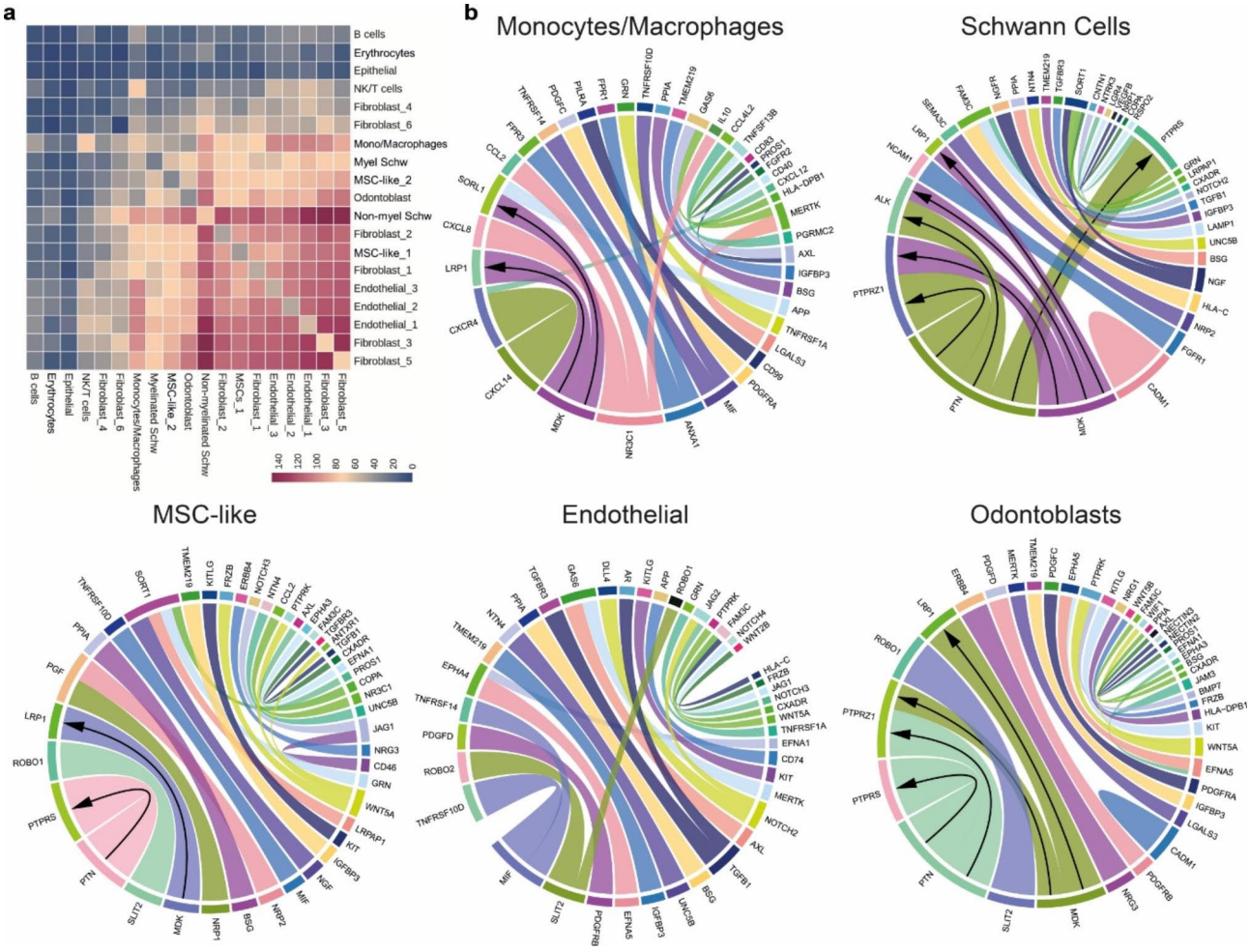

Fig. 4 CellPhoneDB analysis predicted *PTN* and *MDK* interactions in the dental pulp. (**a**) Heatmap showing the total number of statistically significant predictions of cell-cell interactions. (**b**) Chord diagrams of the top 25 ligand-receptor pairs between fibroblasts and their corresponding cell types. Line thickness represents an interaction score obtained from fibroblast clusters involved in the interaction. Arrows indicate *PTN* and *MDK* on fibroblasts and their predicted interacting partners on the predicted target cell type

oral tumors [20]; Cholecystokinin (*CCK*), which regulates calcium transport in organ mineralization [21]. Notably, genes related to nervous system development and neurogenesis were differentially expressed, a finding reiterated by the GO analysis. Receptor-type tyrosine-protein phosphatase delta (*PTPRD*), identified as a critical growth suppressor in the central nervous system (*CNS*) [22]; Neurexin 1 (*NRXN1*), a receptor found in CNS synapses that plays an important role in neural development [8]; Carboxypeptidase A6 (*CPA6*), involved in the processing of neuropeptides and reported to be upregulated in DP [23]. Taken together, these findings are consistent with the ectomesenchymal origin of DP.

The embryological development of craniofacial connective tissues involves neural crest-derived cells that acquired mesenchyme features, and thus are termed ectomesenchymal cells [24]. This neural component of DP tissues remains relevant after development. In adult tissue, peripheral axons comprise 40% of DP volume [25], are the basis for pain processing [26], and participate in immune response [27]. Although neurons cannot be isolated by the tissue digestion techniques applied in the sample processing for scRNA-seq, we were able to show that glial cells alone, myelinated and non-myelinated Schwann cells, comprise 12.39% of the DP cell population. It has been reported that sensory nerves recruit MSC through paracrine signaling [4], our analysis indicate that opposing mechanisms may emerge from DP-resident fibroblasts and glial cells through paracrine regulation.

Among the differentially expressed genes in DP-resident fibroblasts *PTN* appear as the top significant and *MDK* is its highly conserved homologue. Both *PTN* and *MDK* code for biochemically similar proteins that share 45% identity in amino acid sequence and exhibit strong binding to sulfated glycosaminoglycans, including

heparin, heparan sulfate and chondroitin sulfate [15, 17]. Recently, Zhang and co-workers examined the role of *PTN* in DP stem cell maintenance, and, using RNA interference in cultured DP, showed that *PTN* protects DP stem cells from senescence [28]. *MDK* is essential in tooth development, participating in epithelial-mesenchymal interactions, where it is secreted by cells of the dental papilla mesenchyme and captured by epithelial cells [29]. This mechanism was further elucidated in a later report, using dental papilla cells in vitro, where *MDK* could promote cell differentiation into odontoblast-like cells via the modulation of *dspp* [30]. However, the role of *MDK* in the adult healthy DP tissue homeostasis is largely unknown. High expression of *MDK* has been previously identified by microarray screening, but expression levels dropped dramatically when compared to caries conditions [31]. Together, these studies indicate that *MDK* is involved in cell proliferation and differentiation but the circumstances leading to the presence or absence of *MDK* are unclear.

Cell-cell communication predictions indicated that among the top 25 significant pairs, *PTN*/*PTPRZ1* may be especially relevant to understanding DP homeostasis. Upon receptor binding, *PTN* inactivates the intrinsic tyrosine phosphatase activity of *PTPRZ1* [32], affecting several downstream targets that are highly regulated by phosphorylation. These include β-catenin and Fyn kinase [33], which are essential to cell proliferation and differentiation, to cell adhesion and cell motility, and regulation of apoptosis. Similarly, *MDK* binding to *PTPRZ1* is predicted to have analogous effects given their homology [15, 34]. It is known that primary cultures of DP stem cells from explanted adult DP shows a high proliferation rate in vitro [35], however, this is not observed in vivo where cell mitosis is undetectable in homeostasis [36, 37]. Our analysis revealed for the first time that the mechanisms for tissue homeostasis, through which DP controls its extraordinary proliferative and differentiation abilities, may involve *PTN*/*PTPRZ1* binding or their homologues.

As life expectancy has increased, the maintenance, repair, and regeneration of dental tissue has become ever more important. Here we identified *PTN* and *MDK* as previously unappreciated players in DP homeostasis. The extensive receptors for these proteins on Schwann cells, along with the ectomesenchymal origin of DP, imply extensive crosstalk between fibroblasts and nerve cells in the regulation of this tissue. A limitation of this work is that computational predictions reported here must be validated in vitro, which will further refine our understanding of intercellular crosstalk in dental pulp. There is a great need for synthetic molecules capable of targeting DP accurately and precisely. Once the putative mediators of intercellular crosstalk identified here are validated experimentally, a natural next step will be to screen small molecules that can target these proteins. Undoubtedly, the treatment of oral diseases will benefit from the ability to specifically target drugs to DP resident fibroblasts.

Methods

Dataset selection

FASTQ files of single-cell RNA sequencing (scRNA-seq) data were retrieved from published studies [1, 6, 7, 13, 38]. All datasets were generated by the Chromium single-cell gene expression platform from 10x Genomics 5' V1 and 3' (V 2 or V3) to avoid other confounding factors and technical biases. In total, we included nineteen datasets from six different healthy human tissues; nine DP (GSE185222, GSE161267, and GSE146123), two bone marrow (BM) (PRJEB37166), two adipose (ADP) (GSE155960), two lung (PRJEB52292), two skin (PRJNA754272) and two peripheral blood mononuclear cells (PBMC). The DP datasets deposited under the above accession numbers contained both healthy and carious DP data, as well as periodontal tissue data, however only data originated from healthy DP tissue were downloaded for analysis in this study. The two PBMC data were acquired from publicly available datasets at 10x Genomics (Supplementary Table 2).

Data pre-processing and quality control

Raw FASTQ files of each dataset were processed with 10x Genomics Cell Ranger version 7.0.0 and mapped against the human reference genome GRCh38 version 2020-A (GENCODE v32/Ensembl 98). Count matrices were then processed with the Seurat package (version 4.1.1) [39] in R (version 4.2.0). Quality control was performed by excluding the cells expressing mitochondrial genes higher than 10% or those expressing lower than 200 genes or higher than 4,000 genes. Cells that expressed more than 3,500 genes were filtered out for the integration of nine dental pulp datasets. Genes that were detected in fewer than three cells were discarded. Data were normalized by the log normalization method and scaled using the NormalizeData and ScaleData functions in Seurat [39] to yield a total count per cell of 10,000.

Data integration and visualization

Data was integrated by the Seurat integration pipeline [40] using 2,000 high variable gene features across all datasets. The top thirty components from principal component analysis (PCA) were used to calculate a Uniform Manifold Approximation and Projection (UMAP) dimensionality reduction, after which clusters were identified using Louvain algorithm [41] based on a shared nearest neighbor (SNN) in the FindCluster function. Each cluster was manually annotated using cell type markers from the literature and curated markers from CellTypist [9].

Quantifying transcriptomic expression of clusters and pseudo-bulk data

Pseudo-bulk PCA was performed using average gene expression across all cells within a cluster. The union of the top 500 genes having the highest absolute values for PC1 and PC2 were retrieved. The average expressions of these genes were transformed into Z-scores and subsequently used to construct a heatmap comparing gene expression profiles in DP with those of the other five tissues. The PCA plots and heatmaps were constructed using ggplot2 [42] and ComplexHeatmap R packages [43].

Differential gene expression and gene ontology (GO) analysis

Fibroblast clusters were subset from the integrated dataset of the six tissues. Differential gene expression (DE) analysis of fibroblasts in DP and in other tissues was performed by the non-parametric Wilcoxon rank sum test using the FindMarkers function in the Seurat pipeline with gene expression levels before integration. The DE results were visualized by a Volcano plot using the scmisc R package (version 0.8.0). GO enrichment analysis for Biological Processes ontology was performed with the list of DE genes with FDR < 0.05, separating up-regulated and down-regulated genes. This analysis was done using the goana function implemented in the limma package[44] and wrapped for single cell analysis in the scmisc package.

Cell-cell interaction analysis

Interactions between cells were predicted based on the expression levels of ligands and their known interacting partners by CellPhoneDB [16]. A heatmap showing potential interactions between cell types was constructed using the default visualizing function of CellPhoneDB. Dot plots showing the interacting pairs and the levels ligand-receptors expression were produced using the scmisc package. Significant means of ligand-receptor interactions from fibroblast clusters were summed to obtain a total interaction score between fibroblast and other cell types. The top 25 interactions were selected to create an adjacency matrix using the igraph R package [45] which was subsequently used to plot the chord diagrams with the circlize [46] package in R.

Supplementary Information

The online version contains supplementary material available at https://doi.org/10.1186/s12864-023-09265-w.

Additional file 1: Supplementary Table 1.

Additional file 2: Supplementary Fig. 1.

Additional file 3: Supplementary Fig. 2.

Additional file 4: Supplementary Fig. 3.

Additional file 5: Supplementary Fig. 4.

Additional file 6: Supplementary Fig. 5.

Additional file 7: Supplementary Fig. 6.

Additional file 8: Supplementary Fig. 7.

Additional file 9: Supplementary Table 2.

Acknowledgements

The authors thank Jantarika Kumar Arora for single-cell analysis consultancy. We would like to acknowledge the support from the FrontierLab exchange program from Osaka University in enabling this study.

Author contributions

N.J., G.L.A. and D.M.S. contributed to conception, design, data acquisition and interpretation, drafted and critically revised the manuscript. N.J., M.L. and D.D. contributed to data analysis, statistical analysis, drafted and critically revised the manuscript. S.P, P.M., J.I.S. and S.I. contributed to interpretation of results, drafted and critically revised the manuscript. All authors gave their final approval and agreed to be accountable for all aspects of the work.

Funding

This work was partly supported by Grants-in-Aid for Scientific Research (grant number JP20K07538 to D.D. and JP22K21301 to M.L.) from the Japan Society for the Promotion of Science. N.J. was supported by the FrontierLab exchange program of Osaka University and Japan Student Services Organization (JASSO). D.M.S was supported by Japan Agency for Medical Research and Development (AMED), Platform Project for Supporting Drug Discovery and Life Science Research (Basis for Supporting Innovative Drug Discovery and Life Science Research) under JP21am0101108. The funders were not involved in preparing this manuscript.

Availability of data and materials

Code availability: Code to reproduce the analyses described in this manuscript can be accessed via: https://github.com/NatnichaJira/DentalPulp
Database links:
GSE161267 (https://www.ncbi.nlm.nih.gov/geo/query/acc.cgi?acc=GSE185222);
GSE161267 (https://www.ncbi.nlm.nih.gov/geo/query/acc.cgi?acc=GSE161267);
GSE146123 (https://www.ncbi.nlm.nih.gov/geo/query/acc.cgi?acc=GSE146123);
10X Genomics (https://www.10xgenomics.com/resources/datasets);
PRJEB37166 (https://www.ebi.ac.uk/ena/browser/view/PRJEB37166);
GSE155960 (https://www.ncbi.nlm.nih.gov/geo/query/acc.cgi?acc=GSE155960);
PRJEB52292 (https://www.ebi.ac.uk/ena/browser/view/PRJEB52292);
PRJNA754272 (https://www.ebi.ac.uk/ena/browser/view/PRJNA754272).

Declarations

Competing Interest

The authors declare no competing interests.

Ethics approval and consent to participate

Not applicable.

Consent for publication

Not applicable.

Received: 28 December 2022 / Accepted: 21 March 2023
Published online: 06 April 2023

References

1. Krivanek J, Soldatov RA, Kastriti ME, Chontorotzea T, Herdina AN, Petersen J, Szarowska B, Landova M, Matejova VK, Holla LI, et al. Dental cell type atlas reveals stem and differentiated cell types in mouse and human teeth. Nat Commun. 2020;11(1):4816.
2. Sharir A, Marangoni P, Zilionis R, Wan M, Wald T, Hu JK, Kawaguchi K, Castillo-Azofeifa D, Epstein L, Harrington K, et al. A large pool of actively cycling progenitors orchestrates self-renewal and injury repair of an ectodermal appendage. Nat Cell Biol. 2019;21(9):1102–12.
3. Feng J, Mantesso A, De Bari C, Nishiyama A, Sharpe PT. Dual origin of mesenchymal stem cells contributing to organ growth and repair. Proc Natl Acad Sci U S A. 2011;108(16):6503–8.
4. Zhao H, Feng J, Seidel K, Shi S, Klein O, Sharpe P, Chai Y. Secretion of shh by a neurovascular bundle niche supports mesenchymal stem cell homeostasis in the adult mouse incisor. Cell Stem Cell. 2014;14(2):160–73.
5. Krivanek J, Adameyko I, Fried K. Heterogeneity and developmental connections between cell types inhabiting Teeth. Front Physiol. 2017;8:376.
6. Pagella P, de Vargas Roditi L, Stadlinger B, Moor AE, Mitsiadis TA. A single-cell atlas of human teeth. iScience. 2021;24(5):102405.
7. Opasawatchai A, Nguantad S, Sriwilai B, Matangkasombut P, Matangkasombut O, Srisatjaluk R, Charoensawan V. Single-Cell Transcriptomic Profiling of Human Dental Pulp in Sound and Carious Teeth: A Pilot Study. Frontiers in Dental Medicine 2022, 2.
8. Ching MS, Shen Y, Tan WH, Jeste SS, Morrow EM, Chen X, Mukaddes NM, Yoo SY, Hanson E, Hundley R, et al. Deletions of NRXN1 (neurexin-1) predispose to a wide spectrum of developmental disorders. Am J Med Genet B Neuropsychiatr Genet. 2010;153B(4):937–47.
9. Dominguez Conde C, Xu C, Jarvis LB, Rainbow DB, Wells SB, Gomes T, Howlett SK, Suchanek O, Polanski K, King HW, et al. Cross-tissue immune cell analysis reveals tissue-specific features in humans. Science. 2022;376(6594):eabl5197.
10. Bhatheja K, Field J. Schwann cells: origins and role in axonal maintenance and regeneration. Int J Biochem Cell Biol. 2006;38(12):1995–9.
11. Jagalur NB, Ghazvini M, Mandemakers W, Driegen S, Maas A, Jones EA, Jaegle M, Grosveld F, Svaren J, Meijer D. Functional dissection of the Oct6 Schwann cell enhancer reveals an essential role for dimeric Sox10 binding. J Neurosci. 2011;31(23):8585–94.
12. Avolio E, Alvino VV, Ghorbel MT, Campagnolo P. Perivascular cells and tissue engineering: current applications and untapped potential. Pharmacol Ther. 2017;171:83–92.
13. Ahlers JMD, Falckenhayn C, Holzscheck N, Sole-Boldo L, Schutz S, Wenck H, Winnefeld M, Lyko F, Gronniger E, Siracusa A. Single-cell RNA profiling of human skin reveals Age-Related loss of dermal sheath cells and their contribution to a Juvenile phenotype. Front Genet. 2021;12:797747.
14. Deng CC, Hu YF, Zhu DH, Cheng Q, Gu JJ, Feng QL, Zhang LX, Xu YP, Wang D, Rong Z, et al. Single-cell RNA-seq reveals fibroblast heterogeneity and increased mesenchymal fibroblasts in human fibrotic skin diseases. Nat Commun. 2021;12(1):3709.
15. Muramatsu T. Midkine and pleiotrophin: two related proteins involved in development, survival, inflammation and tumorigenesis. J Biochem. 2002;132(3):359–71.
16. Efremova M, Vento-Tormo M, Teichmann SA, Vento-Tormo R. CellPhoneDB: inferring cell-cell communication from combined expression of multi-subunit ligand-receptor complexes. Nat Protoc. 2020;15(4):1484–506.
17. Buechler MB, Pradhan RN, Krishnamurty AT, Cox C, Calviello AK, Wang AW, Yang YA, Tam L, Caothien R, Roose-Girma M, et al. Cross-tissue organization of the fibroblast lineage. Nature. 2021;593(7860):575–9.
18. Yin W, Liu G, Li J, Bian Z. Landscape of Cell Communication in Human Dental Pulp. Small Methods. 2021;5(9):e2100747.
19. Partanen AM, Thesleff I, Ekblom P. Transferrin is required for early tooth morphogenesis. Differentiation. 1984;27(1):59–66.
20. Heikinheimo K, Jee KJ, Niini T, Aalto Y, Happonen RP, Leivo I, Knuutila S. Gene expression profiling of ameloblastoma and human tooth germ by means of a cDNA microarray. J Dent Res. 2002;81(8):525–30.
21. Nurbaeva MK, Eckstein M, Devotta A, Saint-Jeannet JP, Yule DI, Hubbard MJ, Lacruz RS. Evidence that calcium entry into calcium-transporting Dental Enamel cells is regulated by cholecystokinin, acetylcholine and ATP. Front Physiol. 2018;9:801.
22. Veeriah S, Brennan C, Meng S, Singh B, Fagin JA, Solit DB, Paty PB, Rohle D, Vivanco I, Chmielecki J, et al. The tyrosine phosphatase PTPRD is a tumor suppressor that is frequently inactivated and mutated in glioblastoma and other human cancers. Proc Natl Acad Sci U S A. 2009;106(23):9435–40.
23. Gong AX, Zhang JH, Li J, Wu J, Wang L, Miao DS. Comparison of gene expression profiles between dental pulp and periodontal ligament tissues in humans. Int J Mol Med. 2017;40(3):647–60.
24. Chai Y, Jiang X, Ito Y, Bringas P Jr, Han J, Rowitch DH, Soriano P, McMahon AP, Sucov HM. Fate of the mammalian cranial neural crest during tooth and mandibular morphogenesis. Development. 2000;127(8):1671–9.
25. Franca CM, Riggers R, Muschler JL, Widbiller M, Lococo PM, Diogenes A, Bertassoni LE. 3D-Imaging of whole neuronal and vascular networks of the Human Dental Pulp via CLARITY and light sheet Microscopy. Sci Rep. 2019;9(1):10860.
26. Bae YC, Yoshida A. Morphological foundations of pain processing in dental pulp. J Oral Sci. 2020;62(2):126–30.
27. Zhan C, Huang M, Yang X, Hou J. Dental nerves: a neglected mediator of pulpitis. Int Endod J. 2021;54(1):85–99.
28. Zhang L, Xia D, Wang C, Gao F, Hu L, Li J, Jin L. Pleiotrophin attenuates the senescence of dental pulp stem cells. Oral Dis 2021.
29. Mitsiadis TA, Muramatsu T, Muramatsu H, Thesleff I. Midkine (MK), a heparin-binding growth/differentiation factor, is regulated by retinoic acid and epithelial-mesenchymal interactions in the developing mouse tooth, and affects cell proliferation and morphogenesis. J Cell Biol. 1995;129(1):267–81.
30. Park YH, Lee YS, Seo YM, Seo H, Park JS, Bae HS, Park JC. Midkine promotes odontoblast-like differentiation and tertiary dentin formation. J Dent Res. 2020;99(9):1082–91.
31. McLachlan JL, Smith AJ, Bujalska IJ, Cooper PR. Gene expression profiling of pulpal tissue reveals the molecular complexity of dental caries. Biochim Biophys Acta. 2005;1741(3):271–81.
32. Fukada M, Fujikawa A, Chow JP, Ikematsu S, Sakuma S, Noda M. Protein tyrosine phosphatase receptor type Z is inactivated by ligand-induced oligomerization. FEBS Lett. 2006;580(17):4051–6.
33. Pariser H, Perez-Pinera P, Ezquerra L, Herradon G, Deuel TF. Pleiotrophin stimulates tyrosine phosphorylation of beta-adducin through inactivation of the transmembrane receptor protein tyrosine phosphatase beta/zeta. Biochem Biophys Res Commun. 2005;335(1):232–9.
34. Kadomatsu K, Kishida S, Tsubota S. The heparin-binding growth factor midkine: the biological activities and candidate receptors. J Biochem. 2013;153(6):511–21.
35. Huang GT, Gronthos S, Shi S. Mesenchymal stem cells derived from dental tissues vs. those from other sources: their biology and role in regenerative medicine. J Dent Res. 2009;88(9):792–806.
36. Dammaschke T, Stratmann U, Fischer RJ, Sagheri D, Schafer E. Proliferation of rat molar pulp cells after direct pulp capping with dentine adhesive and calcium hydroxide. Clin Oral Investig. 2011;15(4):577–87.
37. Ishikawa Y, Ida-Yonemochi H, Nakakura-Ohshima K, Ohshima H. The relationship between cell proliferation and differentiation and mapping of putative dental pulp stem/progenitor cells during mouse molar development by chasing BrdU-labeling. Cell Tissue Res. 2012;348(1):95–107.
38. Hildreth AD, Ma F, Wong YY, Sun R, Pellegrini M, O'Sullivan TE. Single-cell sequencing of human white adipose tissue identifies new cell states in health and obesity. Nat Immunol. 2021;22(5):639–53.
39. Hao Y, Hao S, Andersen-Nissen E, Mauck WM 3rd, Zheng S, Butler A, Lee MJ, Wilk AJ, Darby C, Zager M, et al. Integrated analysis of multimodal single-cell data. Cell. 2021;184(13):3573–3587e3529.
40. Stuart T, Butler A, Hoffman P, Hafemeister C, Papalexi E, Mauck WM 3rd, Hao Y, Stoeckius M, Smibert P, Satija R. Comprehensive Integration of single-cell data. Cell. 2019;177(7):1888–902. e1821.
41. Blondel VD, Guillaume JL, Lambiotte R, Lefebvre E. Fast unfolding of communities in large networks. J Stat Mech-Theory E 2008.
42. Wickham H. ggplot2: Elegant Graphics for Data Analysis. Use R 2009:1–212.
43. Gu ZG, Eils R, Schlesner M. Complex heatmaps reveal patterns and correlations in multidimensional genomic data. Bioinformatics. 2016;32(18):2847–9.
44. Young MD, Wakefield MJ, Smyth GK, Oshlack A. Gene ontology analysis for RNA-seq: accounting for selection bias. Genome Biol 2010, 11(2).
45. Csardi G, Nepusz T. The igraph software package for complex network research. InterJournal complex systems. 2006;1695(5):1–9.
46. Gu Z, Gu L, Eils R, Schlesner M, Brors B. Circlize implements and enhances circular visualization in R. Bioinformatics. 2014;30(19):2811–2.

Publisher's Note